Vector-Potential Boundary-Integral Evaluation of Eddy–Current Interaction with a Crack

J. R. Bowler, Y. Yoshida, and N. Harfield

Abstract— **In eddy–current nondestructive evaluation, an excitation coil, used to induce current in a conductor, changes impedance in the presence of a crack. The impedance change can be calculated from a knowledge of the coil parameters, the excitation frequency, and the crack geometry. Two boundary integral formulations of the problem are compared. The first formulation uses an electric field integral equation, and the second expresses the magnetic vector potential in integral form using an integral kernel with a weaker singularity. The vector potential formulation, presented here for the first time, leads to a more complicated equation but has a singular kernel that is easier to deal with. In addition, the new approach opens up a number of possibilities for further analytical developments. An example calculation is performed for a long, surface-breaking crack, and the results are compared to available analytical solutions. Very good agreement is found between the numerical solution of the integral equation and the analytical results.**

Index Terms—**Crack, eddy–current, integral equation.**

I. Introduction

CRACKS in metals are frequently irregular, but theoretical predictions of their effects on eddy–currents are tractable using an idealized form of the problem. An ideal crack is one that has a negligible opening, is impenetrable to electric currents, and is defined on a smooth, regular open surface. In a previous study [1], it was stated that such a flaw produces a discontinuity in the electric field of a form that can be reproduced by a surface layer of current dipoles, the dipole orientation being normal to the crack surface. This means that the effect of the crack is the same as an equivalent electric source in that the scattered field may be viewed as being generated by a dipole layer. The main benefit of this approach, apart from its intuitive appeal, is that it reduces a three-dimensional vector field problem to one of finding a single component vector, the dipole density, on a surface. The surface dipole density is determined by a Fredholm integral equation of the first kind. An expression for the driving point impedance of an eddy–current probe due to the crack [1] is derived using a reciprocity theorem [2].

The boundary conditions of an ideal crack are reviewed here along with the electric field integral equation (EFIE) method for computing the scattering at an ideal crack [1]. The EFIE approach is then compared to a vector potential formulation of the same problem leading to a different integral equation for the dipole density.

Eddy–current theory thus gives us a choice between two boundary integral methods. These choices have parallels in ordinary scalar diffraction theory [3] as well as in antenna theory where one has the alternatives of Poklington's electric field or Hallen's vector potential equation for calculating the current in a wire antenna [4], [5].

As in antenna theory, the vector potential formulation leads to an integral equation with a kernel that has a weaker singularity than that of the corresponding electric field integral equation. The hypersingularity in the latter can be dealt with directly using a numerical scheme that interprets the integral operator as a Hadamard finite part [6] following the approach used in [1]. An alternative, and to many the preferred option, is to regularize the integral equation through analytical rather than numerical means. In the process of regularization, the integral equation can be transformed to one where the kernel has a weaker singularity. The new kernel means that the principal value of the singular integral can be used following classical potential theory [7].

The relative merits of the two formulations are not yet fully explored. However, the ability to achieve numerical stability and to control errors in the results are significant considerations. Although these are important issues, they are not considered further in this paper. Instead, we examine the possibility of using the vector potential formulation for calculations where the skin depth is small compared to the characteristic size of a defect. In pursuit of this objective, a link has been made between the vector potential integral equation and the high-frequency limit theories of Auld *et al.* [8] and Michael *et al.* [9]. In the high-frequency limit, the field is determined from solutions of the Laplace equation in two dimensions whose domain is the crack surface. Using the vector potential formulation, it will be shown that the surface Laplacians emerge naturally as the limiting case of an integral equation valid at arbitrary frequencies.

Manuscript received May 6, 1996; revised February 20, 1997. The work of J. R. Bowler was supported by the Ministry of Defense, U.K., and the Defense Research Agency, Farnborough, U.K. The work of Y. Yoshida was supported by the British Council.

J. R. Bowler and N. Harfield are with the Department of Physics, the University of Surrey, Guildford, Surrey GU2 5XH, U.K.

Y. Yoshida is with the Nuclear Engineering Research Laboratory, the University of Tokyo, Ibaraki 319-11, Japan.

Publisher Item Identifier S 0018-9464(97)06158-X.

II. Crack Interface Conditions

Consider an ideal crack defined on an open surface S_0 in a conductor carrying alternating eddy current varying as the real part of $\exp(-i\omega t)$. Because S_0 does not support a singular surface current, the tangential magnetic field is continuous across it. With Δ denoting the difference in field between

adjacent points on opposite faces, this condition is written

$$\Delta \boldsymbol{H}_t = 0. \tag{1}$$

The subscript t refers to components tangential to the surface S_0. For ferromagnetic materials containing a crack with a small opening, (1) may not be an appropriate idealization, but the present analysis is valid for materials whose permeability is that of free space.

Since the magnetic flux density has zero divergence, its normal component, B_n, is continuous at the crack. This condition is written

$$\Delta B_n = 0 \tag{2}$$

at S_0. From (2), together with Faraday's induction law, it can be shown that $\nabla \cdot [\hat{n} \times \Delta \boldsymbol{E}_t] = 0$, $\hat{n}$ being a unit vector normal to S_0. This property of the electric field at the crack surface allows us to write $\Delta \boldsymbol{E}_t$ as the gradient of a surface scalar function. Thus, we introduce a surface scalar function $p(\boldsymbol{r}_0)$, $\boldsymbol{r}_0 \in S_0$, such that

$$\Delta \boldsymbol{E}_t = -\frac{1}{\sigma} \nabla_t p \tag{3}$$

where $\nabla_t = \nabla - \hat{n}(\partial/\partial n)$ is the gradient tangential to S_0, and σ is the conductivity of the material. Equation (3) expresses the jump in the electric field at the crack in terms of a surface function p that we interpret as the current dipole density. The justification for this view is that (3) can be derived by an alternative route, whereby, the discontinuity in the field due to a dipole layer is derived. The derivation applicable to eddy currents is much the same as that used in electrostatics, where charge dipoles give rise to a jump in the electrostatic field [10].

Apart from the above interface conditions, an ideal crack is characterized by a boundary condition that states that the normal component of the electric field at the surface of a crack is zero. This condition is written

$$E_n^{\pm} = 0 \tag{4}$$

where the superscript $\pm$ refers to limiting values as S_0 is approached from one side or the other. The subscript n denotes the component normal to the surface S_0. Equation (4) is based on two assumptions. First, no electric current crosses S_0. Second, current causing charge buildup on the crack faces is negligible. The second assumption implies that displacement current across the crack is negligible compared to the magnitude of charge current flowing around the crack. At typical eddy–current frequencies (<10 MHz), this is a very good approximation unless the crack opening approaches atomic dimensions, in which case (4) must be modified.

III. Electric Field Integral Equation

A suitable dyadic Green's function may be employed to transform the effective source $\boldsymbol{p} = \hat{n}p$ into the scattered electric field [1]. Since $\boldsymbol{p}$ is a surface distribution, it is appropriate that the scattered field is expressed as a surface integral over S_0. The total electric field is then given by

$$\boldsymbol{E}(\boldsymbol{r}) = \boldsymbol{E}^{(i)}(\boldsymbol{r}) + i\omega\mu_0 \int_{S_0} \mathcal{G}(\boldsymbol{r}|\boldsymbol{r}') \cdot \boldsymbol{p}(\boldsymbol{r}')\, dS' \tag{5}$$

where $\boldsymbol{E}^{(i)}(\boldsymbol{r})$ is the incident field. $\mathcal{G}(\boldsymbol{r}|\boldsymbol{r}')$ is an electric dyadic Green's function which satisfies

$$\nabla \times \nabla \times \mathcal{G}(\boldsymbol{r}|\boldsymbol{r}') - k^2 \mathcal{G}(\boldsymbol{r}|\boldsymbol{r}') = \mathcal{I}\delta(\boldsymbol{r} - \boldsymbol{r}') \tag{6}$$

and subject to the same continuity conditions at an air–conductor interface as the electric field. In (6), $\mathcal{I} = \hat{x}\hat{x} + \hat{y}\hat{y} + \hat{z}\hat{z}$ is the unit tensor and $k^2 = i\omega\mu_0\sigma$. The unflawed test piece will be treated as a half-space conductor whose permeability is that of free space. The dyadic Green's function $\mathcal{G}(\boldsymbol{r}|\boldsymbol{r}')$, defined both in air (where $\sigma = 0$) and in the conducting half space, is given in [11]. At the interface in the plane $z = 0$, $\hat{n} \times \mathcal{G}(\boldsymbol{r}|\boldsymbol{r}')$ and $\hat{n} \times \nabla \times \mathcal{G}(\boldsymbol{r}|\boldsymbol{r}')$ are continuous, thus ensuring that the tangential electric and magnetic fields are continuous.

Using the ideal crack boundary condition, (4) in conjunction with (5) gives an integral equation for the dipole density

$$E_n^{(i)}(\boldsymbol{r}^{\pm}) = -i\omega\mu_0 \lim_{\boldsymbol{r} \to \boldsymbol{r}^{\pm}} \int_{S_0} G^{nn}(\boldsymbol{r}^{\pm}|\boldsymbol{r}')p(\boldsymbol{r}')\, dS' \tag{7}$$

where $G^{nn} = \hat{n} \cdot \mathcal{G} \cdot \hat{n}$. A numerical scheme for calculating the dipole density from (7) is given elsewhere [1].

An important attribute of p is that it vanishes at the edge of the crack [12], a property exhibited naturally by the solution of (7). Note that while (7) gives the correct edge behavior automatically, in the following vector potential method the edge conditions must be imposed as an auxiliary condition.

IV. Vector Potential Formulation

A. General Development

In this second approach, a conventional magnetic vector potential is defined such that the magnetic flux density is given by

$$\boldsymbol{B}(\boldsymbol{r}) = \nabla \times \boldsymbol{A}(\boldsymbol{r}) \tag{8}$$

where $\boldsymbol{B}(\boldsymbol{r})$ is the magnetic flux scattered by an ideal crack, and $\boldsymbol{A}(\boldsymbol{r})$ represents the scattered field. Application of the Maxwell–Ampere law in the form $\nabla \times \boldsymbol{H} = \sigma \boldsymbol{E}^{(s)}$ gives the scattered electric field as

$$\boldsymbol{E}^{(s)}(\boldsymbol{r}) = \frac{1}{\mu_0\sigma} \nabla \times \nabla \times \boldsymbol{A}(\boldsymbol{r}). \tag{9}$$

Adding the incident field gives the total electric field in the form

$$\boldsymbol{E}(\boldsymbol{r}) = \boldsymbol{E}^{(i)}(\boldsymbol{r}) + \frac{1}{\mu_0\sigma} \nabla \times \nabla \times \boldsymbol{A}(\boldsymbol{r}) \tag{10}$$

at points in the conductor not on the flaw.

The Lorentz gauge has been chosen which means that, for eddy–current applications, $\nabla \cdot \boldsymbol{A}(\boldsymbol{r}) = \mu_0\sigma\phi(\boldsymbol{r})$ where $\phi(\boldsymbol{r})$ is a scalar potential. Standard analysis following this choice of gauge shows that $\boldsymbol{A}(\boldsymbol{r})$ satisfies the Helmholtz equation

$$(\nabla^2 + k^2)\boldsymbol{A}(\boldsymbol{r}) = 0 \tag{11}$$

in homogeneous regions of the conductor. The formal solution of (11) is written as

$$\boldsymbol{A}(\boldsymbol{r}) = \mu_0 \int_{S_0} \mathcal{G}_A(\boldsymbol{r}|\boldsymbol{r}') \cdot \boldsymbol{p}(\boldsymbol{r}')\, dS' \tag{12}$$

which is a form that allows us to recover the electric field integral equation (5) by using (10). In (12), $\mathcal{G}_A(\boldsymbol{r}|\boldsymbol{r}')$ is the appropriate Green's function for transforming the dipole density into the vector potential. This function is related to the electric field dyadic Green's function by

$$\mathcal{G}(\boldsymbol{r}|\boldsymbol{r}') = \frac{1}{k^2}\nabla\times\nabla\times\mathcal{G}_A(\boldsymbol{r}|\boldsymbol{r}'). \tag{13}$$

For a half-space conductor, the vector potential dyadic Green's function is given by

$$\mathcal{G}_A(\boldsymbol{r}|\boldsymbol{r}') = \mathcal{I}\phi(\boldsymbol{r}|\boldsymbol{r}') + \mathcal{I}'\phi(\boldsymbol{r}|\boldsymbol{r}'') + \frac{1}{k^2}\nabla\times\hat{z}\nabla'\times\hat{z}V(\boldsymbol{r}|\boldsymbol{r}'). \tag{14}$$

where $\mathcal{I}' = \hat{x}\hat{x}+\hat{y}\hat{y}-\hat{z}\hat{z}$ and $\phi(\boldsymbol{r}|\boldsymbol{r}')$ is the unbounded domain scalar Green's function given by

$$\phi(\boldsymbol{r}|\boldsymbol{r}') = \frac{e^{ik|\boldsymbol{r}-\boldsymbol{r}'|}}{4\pi|\boldsymbol{r}-\boldsymbol{r}'|}. \tag{15}$$

The coordinate $\boldsymbol{r}'' = \boldsymbol{r}' - 2\hat{z}z'$ locates an image point corresponding to a point at $\boldsymbol{r}'$ reflected in the plane of the surface of the conductor. Also, a function $V(\boldsymbol{r}|\boldsymbol{r}')$ has been introduced given by

$$V(\boldsymbol{r}|\boldsymbol{r}') = \frac{1}{4\pi^2}\int_{-\infty}^{\infty}\int_{-\infty}^{\infty}\left(\frac{1}{\kappa}-\frac{1}{\gamma}\right)\cdot e^{-\gamma(z+z')+iu(x-x')+iv(y-y')}\,du\,dv \tag{16}$$

where $\kappa^2 = u^2+v^2$ and $\gamma^2 = \kappa^2 - k^2$. By combining (13)–(16), one obtains an explicit expression for the electric field dyadic Green's function [11].

Applying the ideal crack boundary condition given in (4) to (10) gives

$$\left[\nabla_t^2\hat{n} - \frac{\partial}{\partial n}\nabla_t\right]\cdot\boldsymbol{A}(\boldsymbol{r}^{\pm}) = \mu_0 J_n^{(i)}(\boldsymbol{r}^{\pm}) \tag{17}$$

with $J_n^{(i)}(\boldsymbol{r}^{\pm}) = \sigma E_n^{(i)}(\boldsymbol{r}^{\pm})$ being the normal component of incident current at the crack. The second term on the left hand side of this equation leads to complications that can be temporarily put to one side by considering a special case in which $\partial[\nabla_t\cdot\boldsymbol{A}(\boldsymbol{r}^{\pm})]/\partial n$ happens to be zero. In this case, the conductor fills all of space and the crack surface occupies a finite region of a plane.

B. Unbounded Domain

For such a planar crack in an infinite conductor, the magnetic vector potential $\boldsymbol{A}(\boldsymbol{r})$, like its source $\boldsymbol{p}(\boldsymbol{r})$, is directed normal to the crack surface S_0. This is the case because the Helmholtz equation does not couple components of $\boldsymbol{A}(\boldsymbol{r})$, the operator ∇^2 being a scalar operator. Furthermore, without an interface present, there is no possibility of coupling between components through the interface conditions. Therefore, the plane crack gives rise to a surface dipole distribution that is a unidirectional electric source and the vector potential itself is also unidirectional. Thus with only one vector component to consider, $\boldsymbol{A}(\boldsymbol{r}) = \hat{n}A(\boldsymbol{r})$, and

$$\nabla_t^2 A(\boldsymbol{r}^{\pm}) = \mu_0 J_n^{(i)}(\boldsymbol{r}^{\pm}). \tag{18}$$

In (18), the normal component of the vector potential at S_0 is related to the incident current via a two-dimensional (2-D) Poisson equation, but we cannot obtain an explicit solution of the equation directly because the boundary conditions on A at the crack edge are unknown. Instead, (18) is combined with the unbounded domain version of (12) to give

$$\nabla_t^2\int_{S_0}\phi(\boldsymbol{r}^{\pm}|\boldsymbol{r}')p(\boldsymbol{r}')\,dS' = J_n^{(i)}(\boldsymbol{r}^{\pm}). \tag{19}$$

Equation (19) is an integro-differential equation for the dipole density. Integrating (19) over an extended domain gives

$$\mu_0\int_{S_0}\phi(\boldsymbol{r}^{\pm}|\boldsymbol{r}')p(\boldsymbol{r}')\,dS' + \psi(\boldsymbol{r}^{\pm}) = \psi(i)(\boldsymbol{r}^{\pm}) \tag{20}$$

where $\psi(\boldsymbol{r}_0)$ is an unknown function satisfying the 2-D Laplace equation. Thus

$$\nabla_t^2\psi(\boldsymbol{r}_0) = 0. \tag{21}$$

$\psi^{(i)}$ is the particular integral of $J_n^{(i)}$ defined through the relationship[1]

$$\psi^{(i)}(\boldsymbol{r}_0) = \mu_0\nabla_t^{-2}J_n^{(i)}(\boldsymbol{r}_0). \tag{22}$$

Equations (20) and (21) contain two unknown functions which must be found simultaneously to give the dipole density. The function ψ is a solution of the Laplace equation, but the boundary conditions are not available. Instead of using boundary conditions that apply directly to ψ, the solution of the Laplace equation must be chosen such that the dipole density satisfying (20) has the correct behavior at the perimeter of the crack. At the buried edge, the energy dissipated is bounded provided that the dipole density vanishes. For a subsurface crack, this means that the dipole density must be zero along the entire crack perimeter.

A suitable numerical scheme for computing the dipole density may be constructed based on a finite number, say N, of nodes. These are distributed both at the edge of the crack and at suitable places on the crack surface. The dipole density associated with each node will be found. For those nodes at the edge, it is already known that the dipole density is zero. The solution of the Laplace equation, ψ, is expanded in terms of a suitable basis whose expansion coefficients are unknown. By making the number of terms in the expansion equal to the number of edge nodes, the total number of unknowns is the same as the number of nodes. The integral equation is approximated by a discrete form by introducing an interpolation scheme and treating the nodes as collocation points. In this way it is possible to arrive at an $N\times N$ matrix of equations whose solution gives the dipole density at the internal nodes and the expansion coefficients for the approximate solution of the 2-D Laplace equation.

[1]The Poisson equation $\nabla_t f = h$, has a solution of the form $f = P+\phi$, where ψ, the general solution (GS), satisfies the Laplace equation and ψ is the particular integral (PI). It is convenient to express the PI using an inverse Laplacian operator as $P = \nabla_t^{-2}h$.

C. Half-Space Conductor

Before considering further the numerical solution of (20), the theory will be generalized to deal with a surface crack in a half-space. For a surface-breaking crack, the term that was temporarily dropped from (17) is retained, writing its integrated form as

$$\left[\hat{n} - \frac{\dfrac{\partial}{\partial n}\nabla_t}{\nabla_t^2}\right] \cdot \boldsymbol{A}(\boldsymbol{r}^{\pm}) + \psi(\boldsymbol{r}^{\pm}) = \psi^{(i)}(\boldsymbol{r}^{\pm}). \tag{23}$$

Combining this with (12) gives

$$\mu_0 \int_{S_0} G(\boldsymbol{r}^{\pm}|\boldsymbol{r}')p(\boldsymbol{r}')\,dS' + \psi(\boldsymbol{r}^{\pm}) = \psi^{(i)}(\boldsymbol{r}^{\pm}) \tag{24}$$

where

$$G(\boldsymbol{r}|\boldsymbol{r}') = \left[\hat{n} - \frac{\dfrac{\partial}{\partial n}\nabla_t}{\nabla_t^2}\right] \cdot [\mathcal{G}_A(\boldsymbol{r}|\boldsymbol{r}') \cdot \hat{n}]. \tag{25}$$

As before, the dipole density that we seek is zero at the buried edge of the crack. At the intersection between the crack and the conductor surface, a different edge condition must be applied to the dipole density since it will not in general be zero there. Note that the normal component of the electric field is zero at a point inside the conductor in the limit as the point approaches the air–conductor interface. As a consequence and in view of (3), the dipole density satisfies the condition

$$\frac{\partial p}{\partial z} = 0 \tag{26}$$

at points where a perpendicular crack meets the surface of the conductor in the plane $z = 0$.

Note that for a perpendicular crack whose normal is in the x-direction, (14), (16), and (25) combine to give

$$G(\boldsymbol{r}|\boldsymbol{r}') = \phi(\boldsymbol{r}|\boldsymbol{r}') + \phi(\boldsymbol{r}|\boldsymbol{r}'') + \mathcal{V}(\boldsymbol{r}|\boldsymbol{r}') \tag{27}$$

where

$$\begin{aligned}\mathcal{V}(\boldsymbol{r}|\boldsymbol{r}') &= \nabla_t^{-2}\frac{\partial^2}{\partial y^2}V(\boldsymbol{r}|\boldsymbol{r}') \\ &= \frac{1}{4\pi^2}\int_{-\infty}^{\infty}\int_{-\infty}^{\infty}\frac{v^2}{k^2-u^2}\left(\frac{1}{\kappa}-\frac{1}{\gamma}\right) \\ &\quad \cdot e^{-\gamma(z+z')+iu(x-x')+iv(y-y')}\,du\,dv.\end{aligned} \tag{28}$$

Equations (27) and (28) define the kernel to be used in solving (24) for the dipole density on an ideal crack in a half-space conductor.

V. High-Frequency Limit

As the frequency of the excitation increases, the skin depth decreases and hence the range of the interaction between dipoles is reduced. As the dipole interaction becomes more localized, the effects of the Green's kernel (27) representing this interaction becomes more confined to the immediate vicinity of the source point. A useful way of examining the limiting case is to seek a representation of the integral operator in the form of a power series expansion in $(ik)^{-1}$. Suppose the region considered is a few skin depths away from the edge of the crack and from the surface of the conductor. In such regions, the effects of reflection from the interface are negligible and the dipole interaction is represented by integrals of the form

$$h(\boldsymbol{r}) = \int_{S_0} \frac{e^{ik|\boldsymbol{r}-\boldsymbol{r}'|}}{4\pi|\boldsymbol{r}-\boldsymbol{r}'|} f(\boldsymbol{r}')\,dS'$$

where $\boldsymbol{r} \in S_0$ and $\boldsymbol{r}' \in S_0$. Because edge effects are neglected and the range of interaction is small, one can modify the integral by restricting the area of integration to a circular region of radius R_0 about a point whose coordinate is $\boldsymbol{r}$. Thus, we write $\boldsymbol{R} = \boldsymbol{r}' - \boldsymbol{r}$ to give

$$h(\boldsymbol{r}) = \int_0^{2\pi}\int_0^{R_0} \frac{e^{ikR}}{4\pi} f(\boldsymbol{r}+\boldsymbol{R})\,dR\,d\theta$$

where $R_0 \gg \delta$, with δ being the skin depth. As the range of the exponential is effectively limited to a few skin depths, the radial integral can be approximated by setting the upper limit to ∞. Expanding $f(\boldsymbol{r}+\boldsymbol{R})$ as a Taylor series about $\boldsymbol{r}$ and integrating gives

$$h(\boldsymbol{r}) = -\frac{1}{2ik} f(\boldsymbol{r}) + \mathcal{O}([ik]^{-3}). \tag{29}$$

Applying this argument to (24) and noting that $\psi^{(i)}(\boldsymbol{r}^{\pm})$ is negligible over most of the crack, it may be shown that at any point on the crack that is a few skin depths from its perimeter,

$$p(\boldsymbol{r}_0) \simeq \frac{2ik\psi(\boldsymbol{r}_0)}{\mu_0} \tag{30}$$

to a first approximation. This means that, at first order, the dipole density is a solution of the Laplace equation in two dimensions in the domain of the crack surface. Again to first order, the integral operator has the representation

$$\int dS'\phi(\boldsymbol{r},\boldsymbol{r}') \simeq -\frac{1}{2ik}\int dS'\delta(\boldsymbol{r}-\boldsymbol{r}') \tag{31}$$

at points that are at least a few skin depths from the crack perimeter.

VI. Numerical Implementation

The vector potential formulation has been used to calculate the interaction of eddy currents with a surface crack of uniform depth d and infinite length. The crack is subject to an incident electric field that is uniform along its length but varies with distance in the direction normal to the surface of the conductor as

$$E_n^{(i)}(z) = E_0 \exp(ik|z|) \tag{32}$$

where E_0 is the unperturbed electric field at the surface of the conductor. In this problem, the perturbed field varies in two dimensions in a plane perpendicular to the direction of the crack. Approximate analytical solutions are available for both high [13], [14] and low frequencies [15]. Here comparisons are made between the analytical expressions for the dipole density and impedance change due to the crack, and numerical calculations made using boundary elements.

In the 2-D crack problem, the vector potential formulation yields the following integral equation:

$$\mu_0 \int_{-d}^{0} G(z, z')p(z')\,dz' + \alpha z + \beta = \psi^{(i)}(z) \tag{33}$$

where the Green's function is given by

$$G(z, z') = \frac{i}{4} H_0^{(1)}(k|z - z'|) + \frac{i}{4} H_0^{(1)}(k|z + z'|). \tag{34}$$

In addition, the boundary condition on $p(z)$ is expressed as

$$p(-d) = 0 \tag{35}$$

$$\left.\frac{\partial p}{\partial z}\right|_{z=0} = 0. \tag{36}$$

The method of moments is applied to solve (33) numerically. Let us subdivide the crack region, $-d \le z \le 0$, into m sections and denote the z-coordinate of the two edge points of the jth section as z_j and z_{j+1}, where $z_{j+1} - z_j = \Delta z$, $z_1 = -d$ and $z_{m+1} = 0$. Introducing the piecewise linear basis function, the dipole density $p(z)$ is expressed as

$$p(z) = \sum_{j=1}^{m+1} N_j(z)p_j \tag{37}$$

where the basis function is

$$N_j(z) = \begin{cases} 1 - \dfrac{|z - z_j|}{\Delta z}, & \text{if } z_{j-1} < z < z_{j+1} \\ 0, & \text{otherwise} \end{cases} \tag{38}$$

where $j = 1, \cdots, m-2$. A special treatment is needed to impose the Neumann-type boundary condition (36). Here, the quadratic interpolation function is used only in the mth section $[z_m, z_{m+1}]$. Assuming the continuity of the interpolation function and its derivative at z_m and applying (36), we have

$$N_{m-1}(z) = \begin{cases} 1 - \dfrac{|z - z_{m-1}|}{\Delta z}, & \text{if } z_{m-2} < z < z_m \\ \dfrac{z^2 - z_m^2}{2\Delta z^2}, & \text{if } z_m \le z \le z_{m+1} \\ 0, & \text{otherwise} \end{cases} \tag{39}$$

$$N_m(z) = \begin{cases} 1 - \dfrac{|z - z_{m-1}|}{\Delta z}, & \text{if } z_{m-1} < z < z_m \\ 1 - \dfrac{z^2 - z_m^2}{2\Delta z^2}, & \text{if } z_m \le z \le z_{m+1} \\ 0, & \text{otherwise} \end{cases} \tag{40}$$

and $N_{m+1}(z) = 0$. Thus, (37) can be rewritten as

$$p(z) = \sum_{j=2}^{m} N_j(z)p_j \tag{41}$$

where the boundary condition (35) is used.

By applying the point matching method, (33) yields

$$\mu_0 \sum_{j=2}^{m} \int_{-d}^{0} G(z_i, z')N_j(z')p_j\,dz' + \alpha z_i + \beta = \psi^{(i)}(z_i) \tag{42}$$

where z_i is a z-coordinate of ith matching point. When we have $m+1$ matching points, i.e., $\{z_1, z_2, \cdots, z_{m+1}\}$, the following linear algebraic equation system is obtained:

$$[C]\{p\} = \{R\} \tag{43}$$

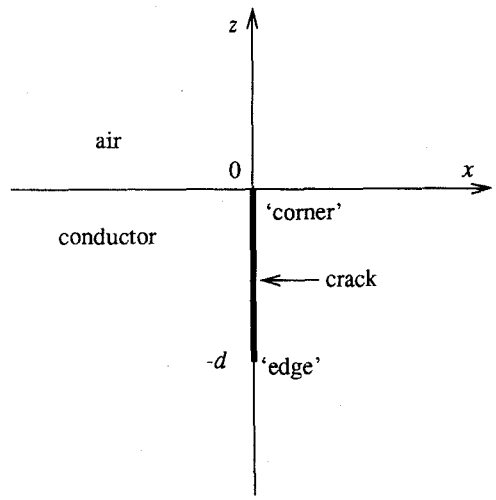

Fig. 1. Geometry for the 2-D problem of a surface-breaking crack of uniform depth.

where

$$\{p\} = \{p_2, p_3, \cdots, p_m, \alpha, \beta\}^T \tag{44}$$

$$\{R\} = \{\psi^{(i)}(z_1), \cdots, \psi^{(i)}(z_{m+1})\}^T \tag{45}$$

and $[C]$ is the $(m+1)$th order square matrix whose components are given by

$$C_{ij} = \begin{cases} \mu_0 \displaystyle\int_{-d}^{0} G(z_i, z')N_{j+1}(z')\,dz', & \text{if } j < m, \\ z_i, & \text{if } j = m, \\ 1, & \text{if } j = m+1. \end{cases} \tag{46}$$

The integral in (46) is evaluated numerically using the Gauss–Legendre quadrature scheme.

VII. Numerical Results

Examples of numerical predictions are presented and compared to analytical solutions for the 2-D problem of a long, surface-breaking crack of uniform depth in a uniform incident field. The geometry is shown in Fig. 1. The incident field is assumed to be $\psi^{(i)} = -\mu_0 H_0 \exp(ik|z|)/ik$, where H_0 is the magnetic field at the conductor surface. The values for conductivity and crack depth used in the computation are 1.0×10^6 Sm^{-1} and 1.0 mm, respectively.

Analytical solutions are available in the high-frequency regime, where the crack depth d is much larger than the skin-depth $\delta = \sqrt{2/\omega\mu_0\sigma}$ (typically, we require $d/\delta \gg 3$ for high-frequency solutions to be valid), for intermediate frequencies (that is, $\frac{3}{2} < d/\delta < 3$) and in the low-frequency regime where $d/\delta \ll 1$. In this section, results of comparisons between numerical calculations and analytical results are made for high and intermediate frequencies. Results for the low-frequency regime are presented elsewhere [15].

A. High-Frequency Regime

In the high-frequency regime, where the crack depth is much larger than the skin depth, an analytical expression for the

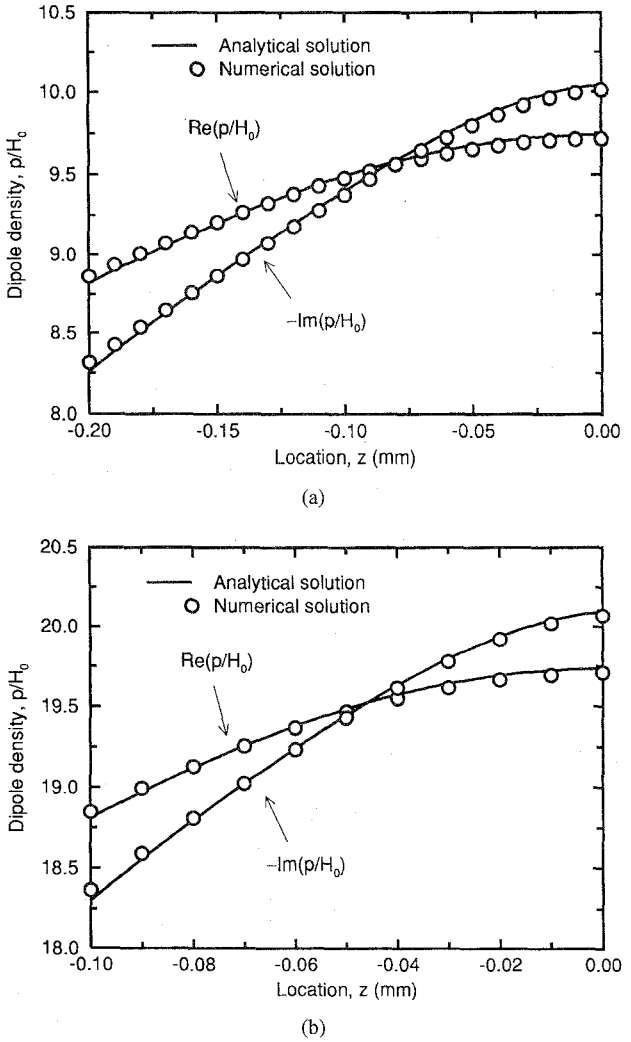

Fig. 2. Comparison of numerical prediction and analytical solution for the dipole density at the crack near the air–conductor interface in the high-frequency regime. (a) $d/\delta = 5$. (b) $d/\delta = 10$.

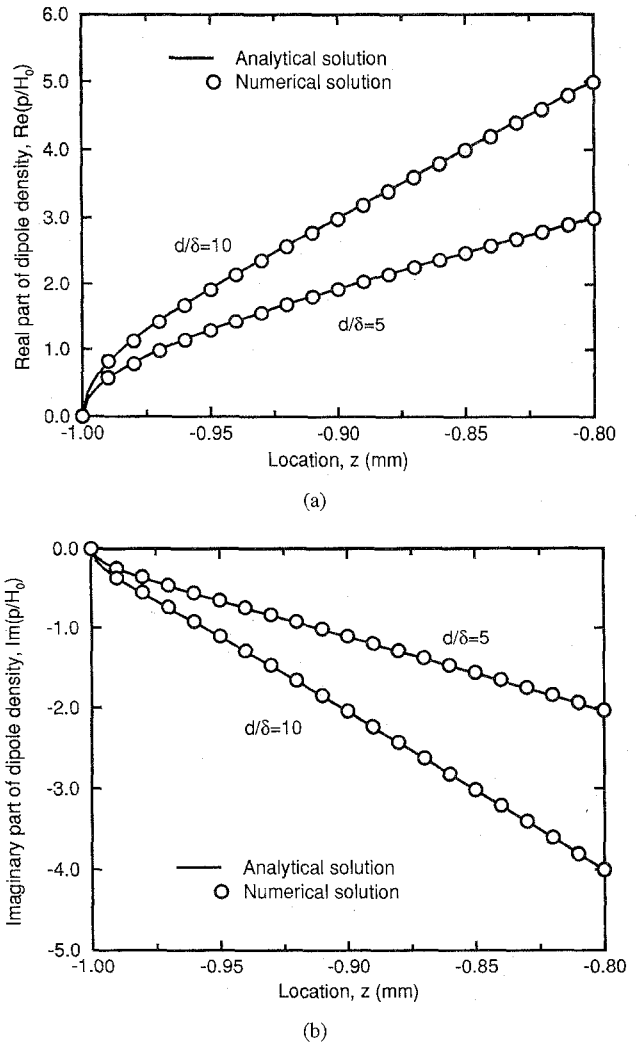

Fig. 3. Comparison of numerical prediction and analytical solution for the dipole density at the crack near its buried edge in the high-frequency regime. (a) Real part of dipole density. (b) Imaginary part of dipole density.

magnetic field valid near the conductor surface is found in [13]. Fig. 2 shows the distribution of the dipole density calculated from this solution in the cases of $d/\delta = 5, 10$. The computed results agree very well with the analytical solution. For the numerical calculation, the crack region was divided into 100 sections. This means that 20 and ten mesh divisions per skin depth were used in the respective computations.

An analytical solution for the fields in the vicinity of the buried crack edge was recently presented in [14]. From this solution, an expression for the current dipole density on the crack near its buried edge can be found:

$$p(\eta) = -H_0\left[(2ik\eta - 1)\,\mathrm{erf}\,(-i\sqrt{ik\eta}\,) + \frac{2i}{\sqrt{\pi}}\sqrt{ik\eta}\,e^{ik\eta}\right] \tag{47}$$

where $\eta = z + d$ and erf (z) is the Gaussian error function. The derivation of (47) is given in the Appendix. Fig. 3 shows the distribution of the dipole density in the cases of $d/\delta = 5, 10$. The computed results agree very well with the analytical solution given in (47).

In the high-frequency limit, the effect of the Green's function becomes concentrated within the vicinity of the source points. In this case we have, corresponding to (30),

$$p(z) \simeq \frac{2ik\psi(z)}{\mu_0}. \tag{48}$$

Fig. 4 shows the comparison of the computed results of the dipole density and $2ik\psi(z)/\mu_0$ in the case of $d/\delta = 10$. It is found that our numerical prediction also demonstrates the validity of (48).

B. Intermediate-Frequency Regime

In the intermediate frequency regime, where $\frac{3}{2} < d/\delta < 3$, an analytical solution for the equivalent current dipole density on the crack is unavailable. It is, however, possible to compare numerically calculated values for the impedance change due to the crack, ΔZ, with the equivalent analytical expressions for this range of skin depths.

The impedance change is computed from dipole density results of the numerical scheme via the following relation, which is derived using the reciprocity theorem [2]:

$$I^2 \Delta Z = -\int_{S_0} \boldsymbol{E}^{(i)}(\boldsymbol{r}) \cdot \boldsymbol{p}(\boldsymbol{r})\, dS. \tag{49}$$

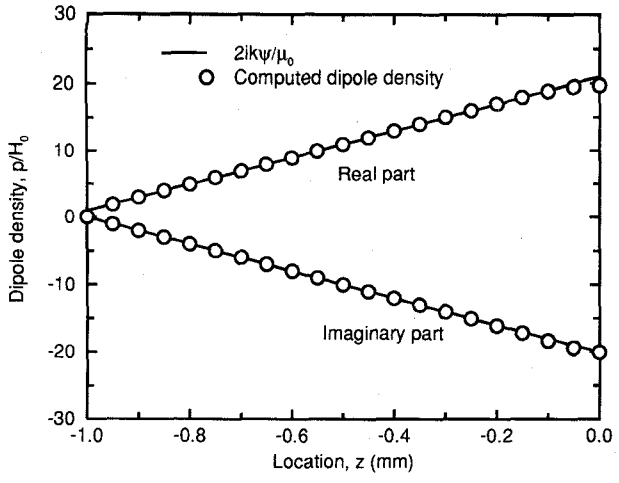

Fig. 4. Comparison of computed dipole density with Laplacian term ($2ik\psi/\mu_0$) in the high-frequency regime.

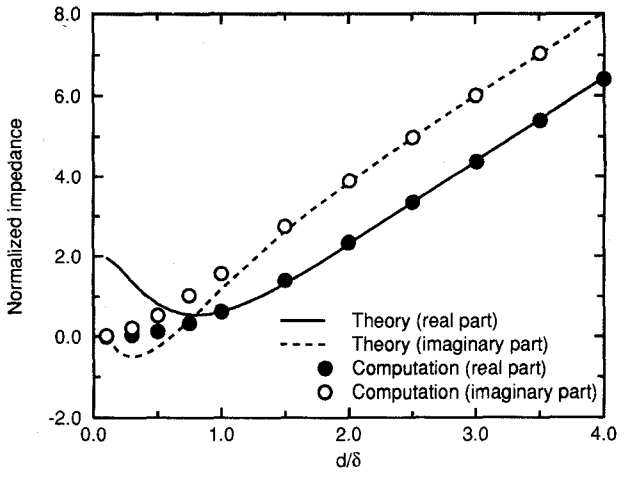

Fig. 5. Comparison of numerical prediction and analytical solution for the impedance change due to the crack in the intermediate- to high-frequency regime.

Two analytical solutions have been presented for this frequency range. The first employs Laplace transforms and the Wiener–Hopf technique [16] and yields a solution in the form of an ordered series in terms of the Laplace transform variables. The second solution method, whose result will be used here, is based on the Geometrical Theory of Diffraction [17]–[19] and yields an approximate solution whose derivation is presented in [20]. The solution builds on that for the thin-skin limit by allowing interaction between the perturbed parts of the field at the crack mouth and edge. These perturbations are assumed to be decoupled in the thin-skin limit. This latter analytical solution is chosen for comparison with the numerical model presented here due to the simpler form of the result. The analytical expression for the impedance change is expressed as a sum of terms

$$\Delta Z = Z_f + Z_e + Z_c \tag{50}$$

where Z_f is the contribution from current flowing uniformly over the crack faces, Z_e is the contribution from the field perturbations at the buried crack edge, and Z_c is the contribution from the fields in the conductor corners near the crack mouth. It is found that [20]

$$Z_f = -\frac{1}{\sigma}\left(\frac{H_0}{I}\right)^2 2ikd \tag{51}$$

$$\begin{aligned} Z_e = -\frac{1}{\sigma}\left(\frac{H_0}{I}\right)^2 \Bigg(&-1-2\sqrt{2}e^{ikd}w\left(\sqrt{2ikd}\right) \\ &- e^{2ikd}\left[(4ikd-1)w\left(\sqrt{2ikd}\right) - \frac{2i}{\sqrt{\pi}}\sqrt{2ikd}\right] \\ &+ [N+(P+1)Q]\left\{\frac{1}{4} - \frac{1}{\sqrt{2}} + e^{ikd}\left[\left(2ikd+\frac{1}{2}\right)\right.\right. \\ &\cdot w\left(\sqrt{2ikd}\right) - \frac{i}{\sqrt{\pi}}\sqrt{2ikd} - 2\Bigg] \\ &+ \frac{e^{2ikd}}{\sqrt{2}}w\left(\sqrt{2ikd}\right) - e^{4ikd}\left[\left(2ikd+\frac{1}{4}\right)\right. \\ &\left.\left.\left. \cdot w\left(\sqrt{4ikd}\right) - \frac{i}{\sqrt{\pi}}\sqrt{ikd}\right]\right\}\Bigg) \end{aligned} \tag{52}$$

where $w(z) = \exp(-z^2)\operatorname{erfc}(-iz)$, $\operatorname{erfc}(z) = 1 - \operatorname{erf}(z)$

$$N = \frac{e^{2ikd}\left[w\left(\sqrt{2ikd}\right) - \frac{i}{\sqrt{\pi}}\frac{1}{\sqrt{2ikd}}\right]}{1 - e^{2ikd}\left[w\left(\sqrt{4ikd}\right) - \frac{i}{\sqrt{\pi}}\frac{1}{\sqrt{4ikd}}\right]} \tag{53}$$

$$P = \frac{e^{2ikd}\left[w\left(\sqrt{4ikd}\right) - \frac{i}{\sqrt{\pi}}\frac{1}{\sqrt{4ikd}}\right]}{1 - e^{2ikd}\left[w\left(\sqrt{4ikd}\right) - \frac{i}{\sqrt{\pi}}\frac{1}{\sqrt{4ikd}}\right]} \tag{54}$$

$$\begin{aligned} Q = 1 - kz\Big\{&H_0^{(1)}(kz) + \frac{\pi}{2}[\mathcal{H}_0(kz)H_1^{(1)}(kz) \\ &- \mathcal{H}_1(kz)H_0^{(1)}(kz)]\Big\} \end{aligned} \tag{55}$$

$H_i^{(1)}(z)$ is the ith-order Hankel function of the first kind, and $\mathcal{H}_i$ is the ith-order Struve function, and

$$\begin{aligned} Z_c \approx -\frac{1}{\sigma}\left(\frac{H_0}{I}\right)^2 \Bigg\{&\frac{8}{\pi} - \sqrt{2}\Bigg[(2ikd+1)\operatorname{erfc}\left(\sqrt{-ikd}\right) \\ &- \frac{2i}{\sqrt{\pi}}\sqrt{ikd}e^{ikd}\Bigg]\Bigg\}. \end{aligned} \tag{56}$$

The above approximate expression for Z_c is used because the full expression (given in [20, eq. (129)]) involves three nested sums and is time consuming to compute.

Fig. 5 shows the comparison between numerically and analytically calculated values for ΔZ. In the numerical calculation, ten mesh divisions per skin-depth were used. There is very good agreement over the range of d/δ for which the analytical solution is valid (for $d/\delta \geq \frac{3}{2}$). For $d/\delta < \frac{3}{2}$, it is clear that the theory for intermediate frequencies breaks down as the low-frequency region is entered.

VIII. Conclusion

The vector potential formulation provides an alternative to the electric field integral equation for calculating the equivalent source of an ideal crack at arbitrary frequencies. Numerical solutions have been found from the vector potential integral

equation using a suitable discretization scheme based on the moment method [21]. Numerical solutions have been compared to approximate analytical results for a 2-D crack problem and very good agreement is found.

The new formulation has been used to show that, in the high-frequency/thin-skin limit, the equivalent source of an ideal crack (the surface dipole density) is, to a first approximation, a solution of the Laplace equation at points away from the edge and mouth of the crack. In the 2-D example considered here, the field at the buried crack edge can, in the high-frequency limit, be approximated by Sommerfeld's solution for diffraction at a half-plane [22]. At the corners where the crack intersects the surface of the conductor, the characteristic corner solutions are found [13].

Appendix
Dipole Density Near the Crack Edge in the Thin-Skin Limit

As explained earlier, the field perturbations due to the crack can be considered as those produced by an equivalent layer of current dipoles p. The dipole density is related to the jump in the tangential component of the electric field across the crack by (3), which can be written

$$E_t^+ - E_t^- = -\frac{1}{\sigma}\nabla_t p \tag{A.1}$$

where the superscripts indicate the limiting values as the crack surface is approached from one side or the other. In the 2-D problem of a long, surface-breaking crack of uniform depth with uniform applied field, described in Section VII, symmetry allows us to write

$$2E_z^+ = -\frac{1}{\sigma}\frac{\partial p_x}{\partial z} \tag{A.2}$$

from which p_x can be calculated if E_z^+ is known. An analytical expression for E_z^+ near the edge of the crack is derived in [14]:

$$E_z^+ = \frac{ikH_0}{\sigma}\left[\operatorname{erf}\left(-i\sqrt{ik\eta}\right) + \frac{i}{\sqrt{\pi}}\frac{e^{ik\eta}}{\sqrt{ik\eta}}\right] \tag{A.3}$$

where $\eta = z + d$ and erf (z) is the Gaussian error function. From (A.2) and (A.3),

$$\begin{aligned} p_x(\eta) &= -2ikH_0\int_0^z \left[\operatorname{erf}\left(-i\sqrt{ik\eta}\right) + \frac{i}{\sqrt{\pi}}\frac{e^{ik\eta}}{\sqrt{ik\eta}}\right]d\eta \\ &= -H_0\left[(2ik\eta - 1)\operatorname{erf}\left(-i\sqrt{ik\eta}\right) + \frac{2i}{\sqrt{\pi}}\sqrt{ik\eta}e^{ik\eta}\right] \end{aligned} \tag{A.4}$$

which is (47) of the main text.

Acknowledgment

The authors would like to acknowledge helpful discussions with Dr. S. Norton of Oak Ridge National Laboratory, TN.

References

[1] J. R. Bowler, "Eddy current interaction with an ideal crack, Part I: The forward problem," *J. Appl. Phys.*, vol. 75, no. 12, pp. 8128–8137, 1994.
[2] R. F. Harrington, *Time Harmonic Electromagnetic Fields.* New York: McGraw-Hill, 1961.
[3] C. J. Bouwkamp, "Diffraction theory," *Rep. Progress Phys.*, vol. 17, pp. 35–100, 1954.
[4] B. P. Popovic, M. B. Drogovic, and A. R. Djordjevic, *Analysis and Synthesis of Wire Antennas.* New York: Wiley, 1982, ch. 1.
[5] M. N. O. Sadiku, *Numerical Techniques in Electromagnetics.* Boca Raton, FL: CRC, 1992.
[6] J. Hadamard, *Lectures on Cauchy's Problem in Linear Partial Differential Equations.* New York: Dover, 1952.
[7] O. D. Kellogg, *Foundations of Potential Theory.* New York: Dover, 1953.
[8] B. A. Auld, F. G. Muennemann, and M. Riaziat, "Quantitative modelling of flaw responses in eddy current testing," in *Research Techniques in Nondestructive Testing,* vol. 7, R. Sharpe, Ed. London, U.K.: Academic, 1984, ch. 2.
[9] D. H. Michael, R. T. Waechter, and R. Collins, "The measurement of surface cracks in metals by using a.c. electric fields," *Proc. Roy. Soc. Lond., A,* vol. 381, pp. 139–157, 1982.
[10] J. A. Stratton, *Electromagnetic Theory.* New York: McGraw-Hill, 1941, p. 191.
[11] J. R. Bowler, S. A. Jenkins, H. A. Sabbagh, and L. D. Sabbagh, "Eddy-current probe impedance due to a volumetric flaw," *J. Appl. Phys.*, vol. 70, no. 3, pp. 1107–1114, 1991.
[12] J. R. Bowler, "Eddy current field theory for a flawed conducting half-space," in *Review of Progress in Quantitative Nondestructive Evaluation,* vol. 5A. New York: Plenum, 1990, pp. 149–155.
[13] A. H. Kahn, R. Spal, and A. Feldman, "Eddy-current losses due to a surface crack in conducting material," *J. Appl. Phys.*, vol. 48, pp. 4454–4459, 1977.
[14] N. Harfield and J. R. Bowler, "Analysis of eddy-current interaction with a surface-breaking crack," *J. Appl. Phys.*, vol. 76, no. 8, pp. 4853–4856, 1994.
[15] N. Harfield, Y. Yoshida, and J. R. Bowler, "Low-frequency perturbation theory in eddy-current nondestructive evaluation," *J. Phys. D: Appl. Phys.*, vol. 80, no. 7, pp. 4090–4100, 1996.
[16] N. Harfield and J. R. Bowler, "Solution of the two-dimensional problem of a crack in a uniform field in eddy-current nondestructive evaluation," *J. Phys. D: Appl. Phys.*, vol. 28, pp. 2197–2205, 1995.
[17] J. B. Keller, "Diffraction by an aperture," *J. Appl. Phys.*, vol. 28, pp. 426–444, 1957.
[18] S. N. Karp and J. B. Keller, "Multiple diffraction by an aperture in a hard screen," *Optica Acta,* vol. 8, pp. 61–72, 1961.
[19] J. B. Keller, "Geometrical theory of diffraction," *J. Opt. Soc. Amer.*, vol. 52, pp. 116–130, 1962.
[20] N. Harfield and J. R. Bowler, "A geometrical theory for eddy-current nondestructive evaluation," *Proc. Roy. Soc. Lond. A,* vol. 453, pp. 1121–1152, 1997.
[21] R. F. Harrington, *Field Computation by Moment Methods.* New York: Macmillan, 1968.
[22] A. Sommerfeld, *Optics.* New York: Academic, 1964.